

Seismic performance analysis of lattice steel - concrete composite column based on ABAQUS

Yun ZOU¹, Jie DING², Cheng-quan WANG¹, Tian-qi LI¹, Xiao-ping FENG¹, Lu CAI²,
Meng-jie XIE²

¹ Professor, Department of Environment and Civil Engineering, Jiangnan University, Jiangsu, China.

² Student, Department of Environment and Civil Engineering, Jiangnan University, Jiangsu, China.

ABSTRACT

On the basis of considering the economic benefit and construction efficiency, this paper puts forward a latticed steel-concrete (LSRC) composite column which is convenient for factory prefabrication. The seismic behavior of a new composite column under low-cycle load is analyzed by ABAQUS software. Seven analysis models are established to analyze the hysteresis performance, skeleton curve, stiffness degradation, ductility and energy dissipation performance of reinforced concrete columns, steel reinforced concrete columns and latticed steel-concrete composite column. Furthermore, the effects of axial compression ratio and concrete strength on the seismic performance of a new type of composite column with angle steel are investigated. Results show that under low-cycle load the latticed steel-concrete composite column has a fusiform curve and good energy dissipation capacity. Under the horizontal load, it also has stronger recovery capacity, and the bearing capacity of the component decreases slightly after failure. The new column has high bearing capacity, compared with the traditional RC column, the displacement ductility of the new column is significantly improved. Compared with the steel reinforced concrete column, it has higher stiffness, more obvious stiffness degradation and more prominent energy dissipation performance. When the strength of concrete is the same, the axial compression ratio has no obvious influence on the seismic performance of the new column. In addition, with the increase of concrete strength, the plastic deformation ability of each new column will be reduced, while the bearing capacity, stiffness and energy dissipation capacity will be obviously improved.

Keywords: latticed steel-concrete composite column, low-cycle load, skeleton curve, hysteresis performance, dissipation capacity.

INTRODUCTION

In recent years, steel reinforced concrete (SRC) columns have been widely used in bridges and building structures due to their advantages of combining steel and concrete effectively. In SRC column, outer concrete can prevent local buckling of steel section. The core steel can effectively enhance the shear capacity of the column and make it have good plastic deformation under earthquake action. Due to its seismic performance, scholars have carried out experimental research on SRC column under low-cycle load at present [1-4], and have achieved results.

In traditional SRC column (see Figure 1a), due to the steel was placed in the center of the column, the flexural capacity cannot be fully exerted. Therefore, scholars have proposed that angle steel should be used instead of steel and placed on the four corners of the rectangular column in order to improve the bending performance of the column as a whole. The ductility of SRC columns is enhanced, and the brittle failure of SRC columns under earthquake is effectively alleviated. Hwang et al. [5] carried out the low-cycle reciprocating test of the four-angle steel column (PSRC), studied the influence of the steel content, stirrup spacing and different structural forms on the seismic performance of the column structure. It is concluded that the ductility of columns under reciprocating load can be enhanced by increasing the thickness of concrete and the section of stirrups. In addition, Hwang et al. [6] have also investigated the effects of the parameters such as the use of bolts in different types of columns, angle steel joints and stirrups on the hysteretic properties of PSRC columns through low-cycle reciprocating tests. The results show that each specimen has good deformation and energy dissipation capacity. By adding stirrups to the outside of angle steel, the premature buckling deformation of angle steel can be prevented, and the ductility of PSRC column under earthquake action can be improved.

This paper proposes a prefabricated lattice steel-concrete (LSRC) composite column (see Figure 1b), which combines the advantages of RC column and SRC column, has economic construction efficiency. In the new column, the four angle steel is placed in the four corners of the section and welded through the steel plate to restrain the core concrete and enhance the overall flexural ability. In order to enhance the restraint performance of the reinforcement, the reinforcement is arranged on the outside to delay the cracking of the outer concrete, and to strengthen the restraint performance of the reinforcement through the two-way tensile reinforcement.

The nonlinear finite element software ABAQUS is used to simulate LSRC columns under low-cycle reciprocating loads. The bearing capacity, stiffness degradation, ductility and energy dissipation of RC, SRC and LSRC columns are compared and analyzed. The effects of different axial compression ratio and concrete strength on the seismic performance of LSRC columns are investigated.

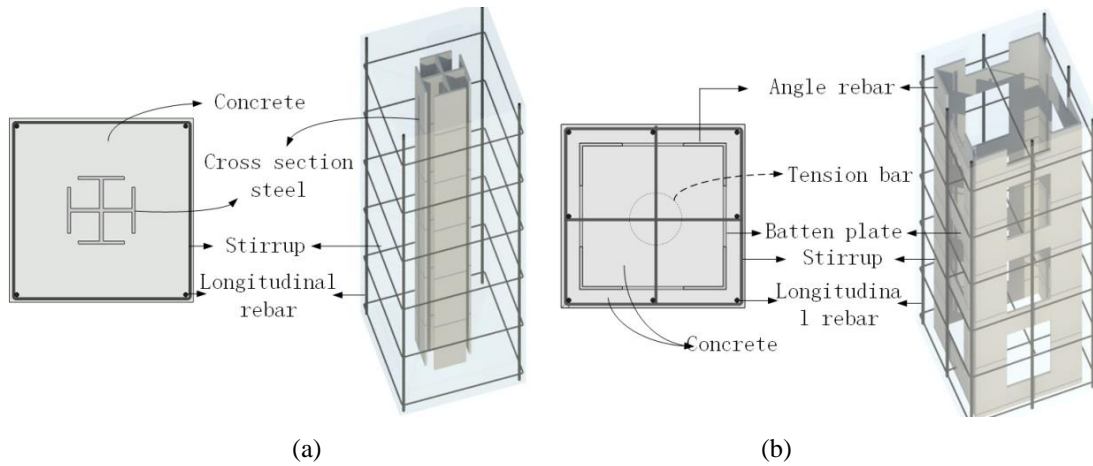


Figure 1. Concrete-encased composite columns: (a) Traditional SRC column, (b) LSRC column.

SPECIMEN SPECIFICATIONS

In this paper, seven specimens were designed to simulate the basic dimensions and details of RC column (S1) and LSRC column (S3~S7) (as shown in Figure 2). The axial pressure ratios of S4 and S5 were 0.4 and 0.2 respectively, and the rest specimens were 0.6 respectively. The height of each specimen was 7,140mm, the size of sections was 600×600mm, and the steel content of sections was 3%. For S1 column, sixteen rebars with diameter of 28mm were used for longitudinal reinforcement, and the rebars with diameter of 8mm were used for hoop and tensile reinforcements, with spacing of 200mm. The three were connected by tying and placed in the center of the column. The section steel of S2 column was placed at the center of the column. The concrete size was shown in Figure 1b. Four longitudinal bars with diameter 14mm were placed in the four corners of the column section, and the stirrups were bound around the column. The diameter of stirrups was 8mm and the spacing was 200mm. For the S3~S7 column, the lattice steel skeleton was formed by welding the quadrangular angle steel and the flat wear plate. The dimension of the angle steel was L-140x140x10, and the lateral reinforcement cage was formed by the longitudinal and hoop reinforcements with diameters of 14mm and 8mm respectively. The diameter of the tensile reinforcement was 8mm, and the spacing in the same direction was 400mm. The concrete strength of specimens S1~S5 was C30, while that of specimens S6~S7 was C40 and C50, respectively. All specimens were made of Q345 steel, longitudinal reinforcement used HRB335 level, stirrups used HPB300 level.

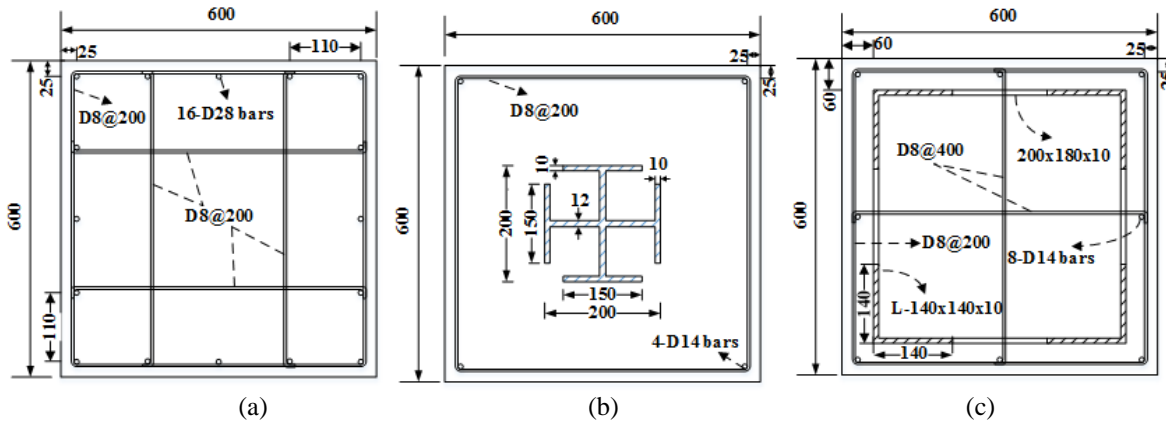


Figure 2. Size and detail structure of specimens: (a) RC column, (b) SRC column, (c) LSRC column.

FINITE ELEMENT MODELING

Material model

Concrete adopted plastic damage model with expansion angle of 30° , eccentricity ratio was 0.1, $f_{b0}/f_{c0} = 1.16$, $K=0.6667$, the viscosity coefficient was 0.002. The stress-strain relationship of concrete subjected to tension and compression adopted the model recommended by Code for Design of Concrete Structures (GB50010-2010) [7], as shown in Figure 3a. In the figure, f_t^* is the uniaxial tensile strength of concrete; ε_t is the peak tensile strain of concrete corresponding to the uniaxial tensile strength f_t^* ; f_c^* is the uniaxial strength of concrete; ε_c is the peak compressive strain of concrete corresponding to the uniaxial compressive strength f_c^* . The elastic modulus and compressive strength of concrete are evaluated according to the test results and the poisson ratio is 0.2.

In all specimen models, the stress and strain relationships of lattice steels, sectional steels and rebar all adopted the ideal elastic-plastic model, as shown in Figure 3b. The constitutive expression was as follows:

$$\sigma = \begin{cases} E_s \varepsilon, & \varepsilon \leq \varepsilon_y \\ f_y, & \varepsilon > \varepsilon_y \end{cases} \quad (1)$$

Among them, E_s is the elastic modulus of steel, f_y is the yield strength of steel, ε_y is the strain corresponding to the yield strength of steel, σ , ε is the stress and strain of steel. The measured yield strength and elastic modulus of steel are 0.3.

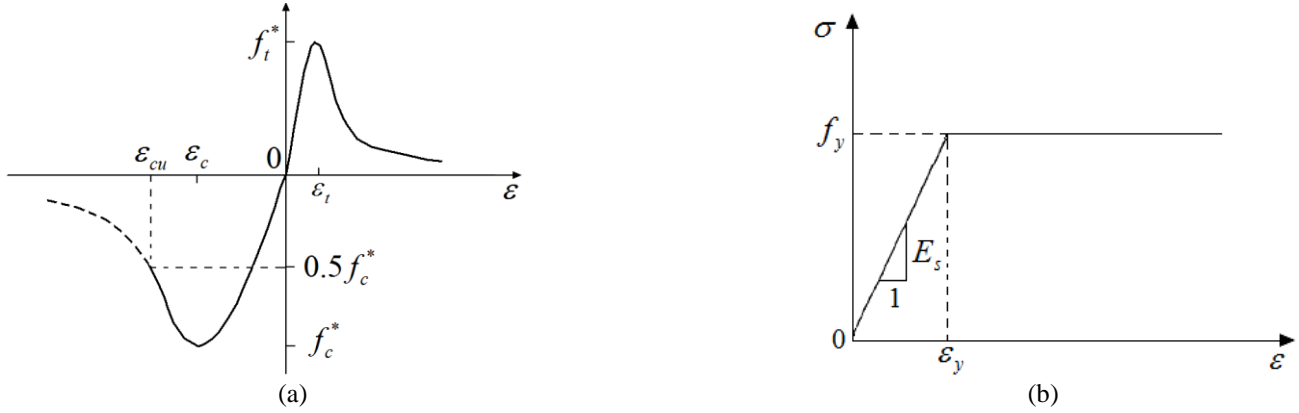


Figure 3. Stress-strain curves of materials: (a) The σ - ε curve of concrete, (b) The σ - ε curve of steel.

Finite element modeling

In this paper, all specimens were simulated with ABAQUS, a large finite element software. Cell selection and grid division: linear components all adopt the 8-node solid unit with three translation degrees of freedom attach node (C3D8R), which has efficient and accurate calculation. And the grid division is conducted by using structured grid division technology. Truss element (T3D2) is the linear components can only withstand tensile and compressive loads in space, which is used to simulate the longitudinal rebars and stirrups. The cell grid model after partitioning is shown in Figure 4.

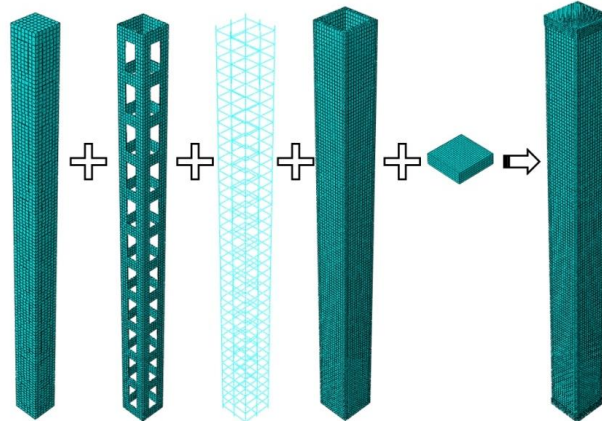


Figure 4. Finite element model

Interaction relationship: the contact relationship between lattice steel and concrete is defined as hard contact upward in normal terms, that is, when the interface is in contact, corresponding stresses can be transferred between the contact surfaces according to the constraint conditions. The penalty function is used to simulate the friction relation of contact surface on tangential upward, and the slip coefficient is set to 0.4. For the S3~S7 column, binding constraints are adopted between core concrete and outsourced concrete. All the specimen models adopted Embed constraint to embed the steel bar into the concrete and establish the joint relationship between the embedded unit and the main unit. Tie constraints are used to bind the steel cap to the column model.

Load and boundary: coupling constraints are established on the steel cap at the top of the column, and concentrated load is applied to the reference point. The load value is derived from the formula $N = n \times (A_s \cdot f_y + A_c \cdot f_c)$. Where n is the axial pressure ratio, A_s , A_c are the section area of steel and concrete respectively, f_y , f_c are their corresponding yield strength and compressive strength respectively. After the axial pressure is applied, the overburden load is applied to the reference point,

and the displacement loading is adopted. The loading curve is shown in Figure 5. The geometrical deformation is considered in the loading process and the complete constraint is set on the bottom of the column.

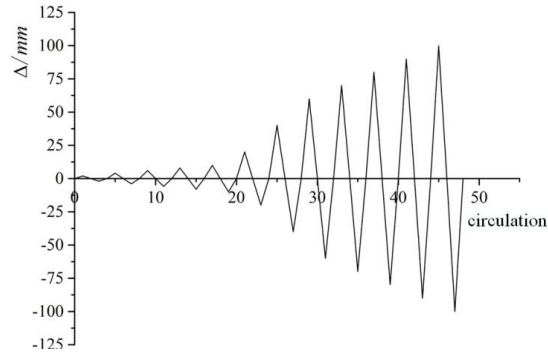


Figure 5. The loading system

ANALYSIS OF FINITE ELEMENT RESULTS

Hysteresis performance

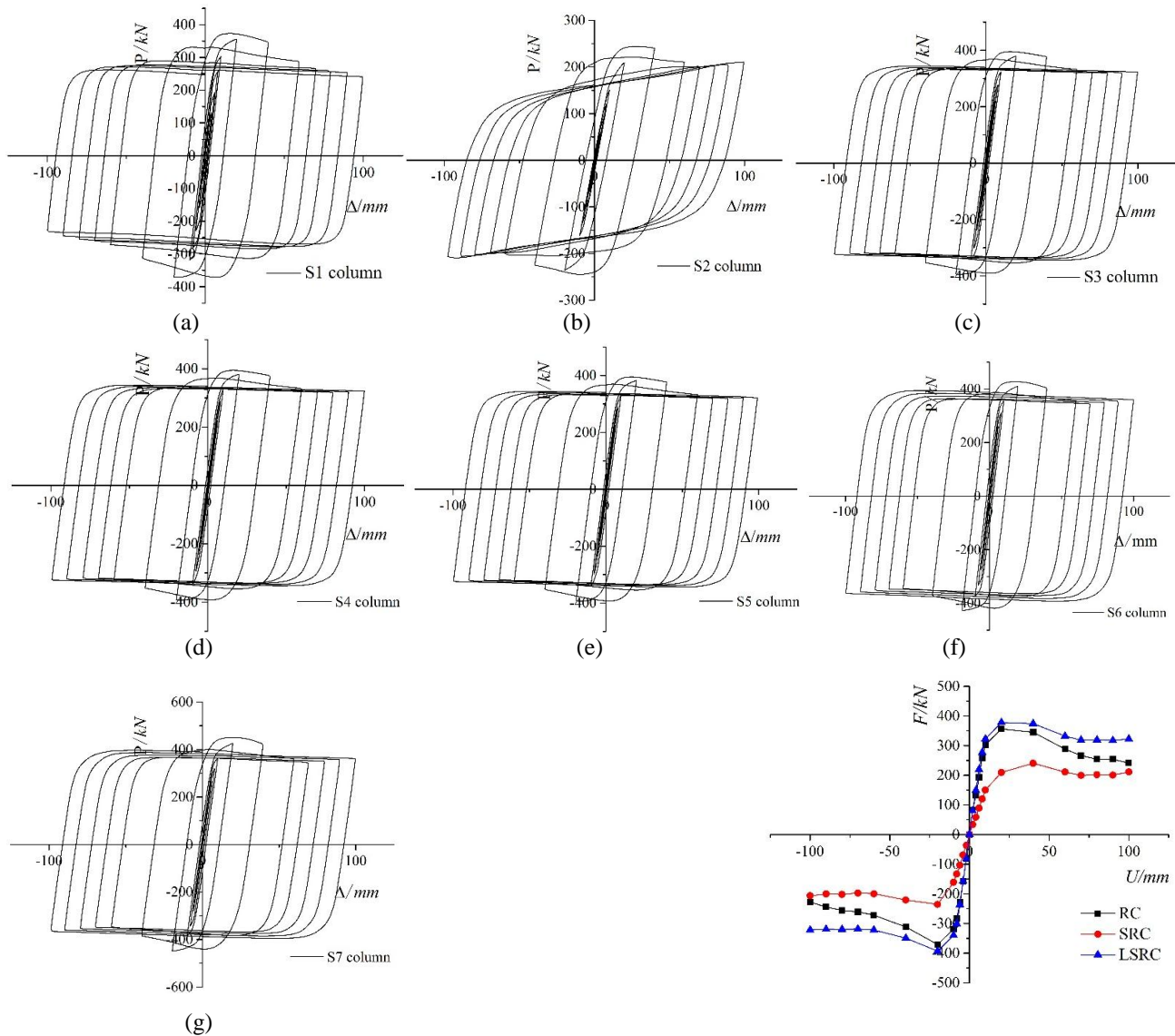


Figure 6. Hysteretic curve of S1~S7

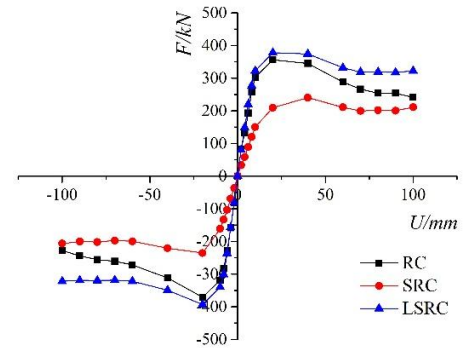


Figure 7. Skeleton curve of S1~S3

The hysteretic curves which are obtained by numerical simulation of the load and displacement of each specimen model under the action of horizontal nappe are shown in Figure 6. It can be seen that the hysteretic curves of S1~S7 are generally fusiform without pinching. Compared with S2, the hysteretic curves of the other specimen models are fuller, and the structural plastic deformation capacity is stronger. This is because the stress distribution of RC column and LSRC column is more uniform under the action of tensile reinforcement, and their overall energy dissipation is better than that of SRC column. At the initial stage of loading, the load-displacement curve was linear due to small horizontal load, and the model columns were in elastic working state. When the loading level reached 20mm, the model column began to yield, and obvious residual deformation occurred. The average value of the pushdown residual deformation of S1 was 11.37mm, and that of S2 was 7.72mm, which reduced by 32.1%, while that of S3 was 10.84mm, which reduced by 4.66%. After each model column reached the ultimate bearing capacity, the whole column was damaged, and the bearing capacity decreased. However, due to the existence of shaped and lattice steels in the SRC and LSRC columns, the bearing capacity increased in the later stage.

Skeleton curve

Figure 7 shows the skeleton curve contrast diagrams of RC, SRC and LSRC columns under the same axial compression ratio and concrete strength. It can be seen from the figure that the variation trend of the three skeleton curves is inverted S-type, and the mechanical characteristics of models under low-cycle load can be divided into the elastic stage, the plastic stage and the failure stage. At the elastic stage, the initial stiffness of S1 and S3 tends to be the same, both greater than that of S2. As the loading level increases, the yield of each model begins to appear. The yield point is obtained according to the principle of energy equivalence in reference [8]. It can be seen that the mean yield load of S3 in the process of horizontal overburden is 331.37kN, which is 6.18% higher than S1 column and 53.04% higher than S2 column. This indicates that the placement of steel mesh in LSRC column effectively delays the cracking of outsourced concrete and restricts the early buckling of lattice steel. When the horizontal displacement is 19.91mm, S3 column reaches the peak load state, and the average value of its ultimate bearing capacity is 385.78kN, which is 5.7% higher than S1 column and 38.3% higher than S2 column, indicating that LSRC column has good flexural bearing capacity under the horizontal load.

Ductility

Ductility coefficient, as one of the important indexes for judging the seismic performance of structures, is an important parameter used to characterize the deformation capacity of structures in the later stage. According to the literature [9], the coefficient of displacement ductility is:

$$\mu = \frac{\Delta_u}{\Delta_y} \quad (2)$$

Among them, Δ_u is the displacement value corresponding to the decrease of bearing capacity to 85% of the peak load, Δ_y is the displacement corresponding to the yield load.

The specific values of bearing capacity and displacement ductility coefficient of S1~S3 can be obtained from Table 1. It can be seen from the table that both the yield displacement and the ultimate displacement of models are smaller than that of the forward loading under the reverse loading. The yield displacement of S1~S3 is basically the same. Compared with S1, the limit displacement of S2 increased by 24.94% and that of S3 increased by 21.23%. It can be seen from the table that the ductility coefficient of S1 is the smallest, with an increase of 26.93% in the ratio of S2 and 23.99% in the ratio of S3 to S1, this is mainly because the internal shape steel and lattice steel enhance the overall ductility of the structure.

Table.1 Yield displacement, limit displacement and ductility factor of each specimen

Specimen number	$+\Delta_y/\text{mm}$	$-\Delta_y/\text{mm}$	$+\Delta_u/\text{mm}$	$-\Delta_u/\text{mm}$	Δ_y/mm	Δ_u/mm	μ
S1	9.98	-9.82	54.97	-38.51	9.9	46.74	4.72
S2	9.83	-9.46	65.27	-59.26	9.64	62.27	6.46
S3	9.82	-9.30	67.31	-51.37	9.56	59.34	6.21

Note: Δ_y and Δ_u are the average of the corresponding displacement in both positive and negative directions

Stiffness degradation

Ring stiffness K_j under the same load level is adopted To represent the stiffness degradation. Since each stage of the model in this paper only cycles once, the expression can be written as follows:

$$K_j = \frac{F_j^1}{\Delta_j^1} \quad (3)$$

Where, F_j^1 is the peak load under j-level loading, Δ_j^1 is the deformation value corresponding to the peak load under j-level loading.

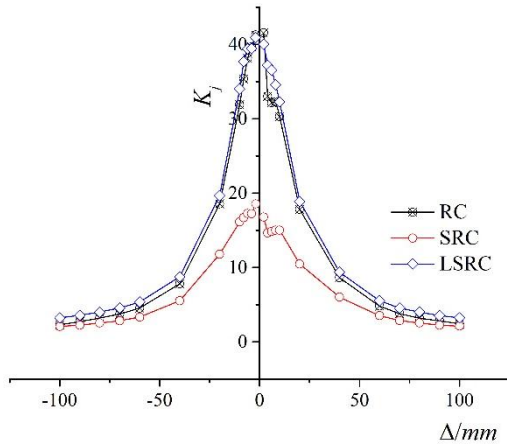


Figure 8. Stiffness degradation curve of S1~S3

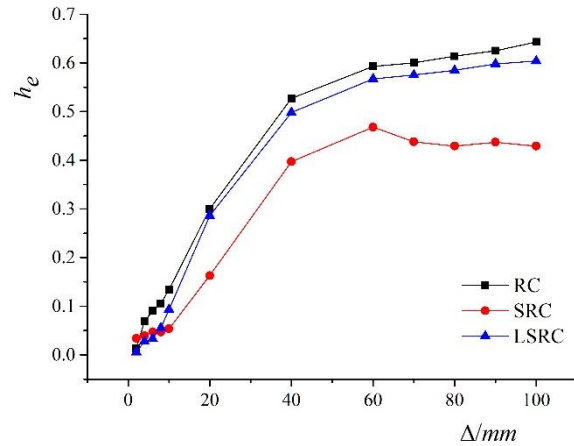


Figure 9. Energy dissipation curves of S1~S3

Figure 8 shows the stiffness degradation curves of RC, SRC and LSRC columns under tipping load. As can be seen from the figure, the initial stiffness of SRC column is the lowest, 18.5kN/mm, the ratio of RC column increased by 54.77%, and that of LSRC column increased by 54.43%, indicating that moving the core area section steel to the quadrangle would significantly improve the initial lateral stiffness of the column. When the column is loaded with positive horizontal displacement, the stiffness of RC and SRC columns declines slowly under low horizontal displacement and the lateral displacement reaches 20mm, the stiffness degradation is more obvious. However, no stiffness mutation occurred in the elastic and plastic stage of LSRC column, indicating that the variation trend of stiffness in the early stage of LSRC column is relatively stable. After reaching the peak load, the stiffness degradation becomes slow and steady. In general, the stiffness under loading of RC and LSRC columns at all levels is greater than that of SRC column, and the stiffness degradation is more obvious.

Energy dissipation

The equivalent damping ratio h_e is used to measure the energy efficiency of specimens under various cyclic loads, the formula is as follows:

$$h_e = \frac{1}{2\pi} \cdot \frac{A_j}{P\Delta} \quad (4)$$

Among them, A_j is the area of the corresponding hysteresis loop under the j-level loading, $P\Delta$ is 1/2 of the product of the peak load on both left and right ends of the hysteresis ring with the corresponding displacement. The greater the value h_e is, the greater the energy dissipation efficiency of components under various loading conditions is. Figure 9 shows the variation curve of the energy dissipation coefficient of specimens S1~S3 under the loading of different horizontal displacement. It can be seen from the figure that when the specimens are in the elastic stage, the equivalent damping ratio of LSRC column is the lowest, followed by SRC column, and the energy dissipation efficiency of LSRC column is the greatest. When the specimens yield as a whole, the bending capacity of LSRC column is fully developed, and the limb angle steel produces large plastic deformation, so its energy dissipation capacity is gradually greater than SRC column. Compared with LSRC column, the constraint effect of RC column on core concrete is poorer. Under constant axial force, lateral expansion of RC column accelerates the annular deformation and yield of internal reinforcement and enhances its plastic energy dissipation capacity. Therefore, the overall energy dissipation efficiency of RC column is slightly greater than that of LSRC column.

PARAMETER ANALYSIS

Skeleton curve

The load-displacement skeleton curve of specimens S3~S7 is shown in Figure 10. It can be seen that all the specimen models experience elastic, plastic and failure stages, and the declining section of the skeleton curve of the specimen is relatively gentle, indicating that it has good ductility. In the diagram, the corresponding axial compression ratios of S3, S4 and S5 specimens are respectively 0.6, 0.4 and 0.2, and the concrete strength is all C30. It can be seen from the figure that the skeleton curve of the S1~S3 specimen is basically consistent. With the decrease of the axial pressure ratio, the S4 yield load and ultimate load increased by 0.77% and 0.37%, respectively, compared with the S3 specimen, the S5 yield value increased by 0.53%, and the limit value decreased by 0.42%, indicating that the bearing capacity of the LSRC column has little impact

on the axial pressure ratio. In addition, it can also be seen from the figure that under the same axial pressure ratio, compared with S3, the bearing capacity of S6 column increased by 8.7% and 7.8%, respectively, and S7 increased by 2.6% and 4.0%, respectively, indicating that reasonable improvement of concrete strength can improve the bearing capacity of specimens.

Ductility coefficient

Figure 11 shows the S3~S7 contrast analysis of ductility coefficient can be seen from the figure of S3~S5 specimen, with the decrease of the axial compression ratio, displacement ductility coefficient decreases 2.3% first, then increased by 3.7%, this is because when the axial compression ratio of 0.6, specimens under axial force some steel yield have occurred, and the plastic deformation capacity slightly higher than the S4 column. In addition, it can be seen from the figure that compared with S3 column, the ductility coefficient of S6 column is reduced by 7.2%, and S7 is reduced by 6.3% compared with S6 column. This indicates that with the increase of concrete strength, the ductility of components gradually decreases, which weakens their plastic deformation capacity.

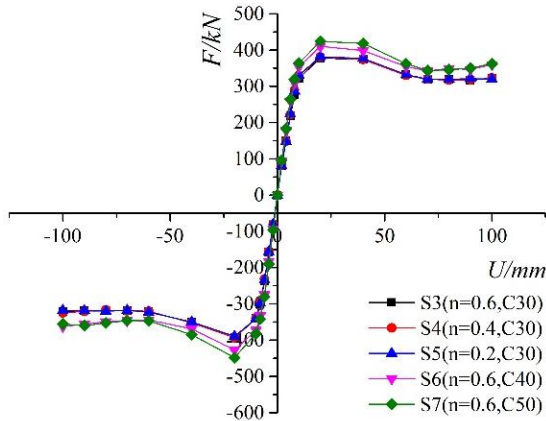


Figure 10. Skeleton curve of S3~S7

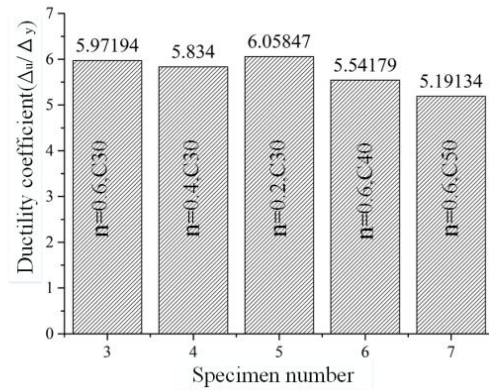


Figure 11. Ductility factor of S3~S7

Stiffness degradation

Figure 12 shows the mean values of positive and negative stiffness degradation curves of S3~S7 specimens under lateral overburden. It can be seen from the figure that in the elastic stage, the stiffness changes of each specimen are different under different axial pressure ratios, indicating that the stiffness degradation of LSRC columns at the early stage is disturbed by axial compression ratio. After entering the plastic deformation, the stiffness degradation curve of the S3~S5 specimen is basically consistent. With the yield of the lattice steel, the specimen produces large plastic deformation, so the stiffness decreases rapidly. After the failure, the rigidity change tends to be flat, showing good ductility. In the figure, S3, S6 and S7 reflect the degradation of the stiffness of specimens with different concrete strength. It can be seen that the stiffness increases with the rise of concrete strength and the increase amplitude gradually decreases. With the increase of horizontal displacement, the stiffness difference gradually decreases, and finally tends to be consistent.

Energy dissipation capacity

The envelope area of hysteretic loop corresponding to the ultimate bearing capacity is adopted to measure the energy dissipation performance of components, the specific energy dissipation of S3~S7 column is shown in Figure 13. It can be seen that when the axial pressure ratio is 0.4, the component energy dissipation ratio increases by 0.22% compared with S3 column; when the axial pressure ratio drops to 0.2, S5 decreases by 0.33% compared with S4. When the axial compression ratio is 0.6, with the improvement of concrete strength, the energy dissipation capacity of sample S6 increases by 7.4% compared with S3 and 3.3% compared with S6, indicating that the improvement of concrete strength helps to improve the energy dissipation performance. Therefore, in actual engineering, LSRC column with higher concrete strength should be used and proper axial compression ratio should be selected to meet the energy consumption demand.

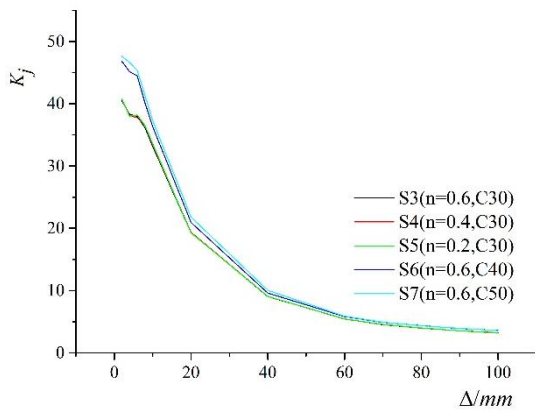


Figure 12. Average stiffness degradation curve of S3~S7

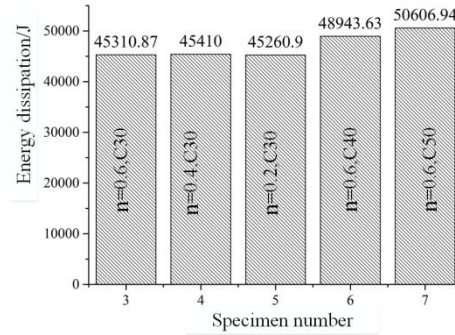


Figure 13. Energy dissipation at load level of 40mm of S3~S7

CONCLUSIONS

By using ABAQUS software, seven finite element models are established to compare and analyze the hysteretic performance, skeleton curve, ductility and stiffness of RC, SRC and LSRC columns, and explore the influence of axial pressure ratio and concrete strength on the seismic performance of LSRC columns. The conclusions are as follows:

- (1) Compared with RC column and SRC column, LSRC column has better bearing capacity, and can withstand higher horizontal load under seismic action. The displacement ductility coefficient of LSRC is higher than that of RC column.
- (2) Compared with traditional RC and SRC columns with steel content, the stiffness of LSRC columns at the elastic and plastic stage is significantly improved, and the stiffness degradation is more obvious, the stiffness variation trend is more stable in the initial loading process.
- (3) The bearing capacity, stiffness, ductility and energy dissipation with the same concrete strength under different axial compression ratios are not significantly different, and the high axial compression ratio will adversely slightly affect the seismic performance. Reasonable improvement of concrete strength can help improve the performances of specimens. With the increase of concrete strength, the ductility of components gradually decreases and the plastic deformation capacity becomes weaker.

ACKNOWLEDGMENTS

This research was supported by the Jiangsu provincial science and Technology Governmental Social Development Project (BE2018625), 2016 Jiangsu provincial construction industry modernization base project and the National Natural Science Foundation of China (51378240), as well as by 2015 Jiangsu provincial building energy saving and construction industry science and technology project.

REFERENCES

- [1] ZENG Lei, TU Xiang, XU Cheng-xiang, et al. (2013). "Experimental study on seismic behavior of steel reinforced concrete columns with unsymmetrical steel cross-sections". *Journal of Building Structures*, 34(03):141-151.
- [2] XU Yong, ZHOU Cui-ying, LIU Ai-rong, et al. (2015). "Experimental study on the seismic behavior of SRC columns under strong aftershocks". *Earthquake engineering and engineering shock*, 35(05):167-172.
- [3] DENG Ming-ke, BU Xing-xing, PAN Jiao-jiao, et al. (2017). "Experimental study on seismic behavior of steel reinforced high ductility concrete short columns". *Engineering Mechanics*, 34(01):163-170.
- [4] WENG Xiao-hong, SHAO Yong-jian, LAO Yu-hua, et al. (2017). "Experimental study on seismic behavior of steel reinforced column under combined torsion". *Journal of Building Structures*, 38(11), 23-33.
- [5] Hyeon-Jong Hwang, Tae-Sung, Hong-Gun Park, et al. (2016). "Axial load and cyclic lateral load tests for composite columns with steel angels". *Journal of Structural Engineering*, 142(5): 1-11.
- [6] Hyeon-Jong Hwang, Tae-Sung, Hong-Gun Park, et al. (2013). "Cyclic loading tests for prefabricated composite columns using steel angle and reinforcing bar". *Journal of Korean society of steel construction*, 25(6):635-647.
- [7] GB50010-2010, (2010). "Code for design of concrete structures". Beijing: China Architecture & Building Press.
- [8] DONG Hong-ying, LI Jian-rui, CAO Wan-ling, et al. (2016). "Axial compression performance of rectangular concrete-filled steel tubular columns with different cell details". *Journal of Building Structures*, 37(05):69-81.
- [9] QING Peng. (2015). "Study on seismic behavior of concrete-filled steel tubular column with CFRP". Hunan: Hunan University.